

High-precision microscopic phase imaging without phase unwrapping for cancer cell identification

Eriko Watanabe,^{1,*} Takashi Hoshiba,² and Bahram Javidi³

¹Center for Frontier Science and Engineering, The University of Electro-Communications, Tokyo 182-8585, Japan

²Department of Biochemical Engineering, Graduate School of Science and Engineering, Yamagata University, Yamagata 992-8510, Japan

³Electrical & Computer Engineering Department, University of Connecticut, Storrs, Connecticut 06269-4157, USA

*Corresponding author: eriko@ee.uec.ac.jp

Received October 22, 2012; revised January 24, 2013; accepted January 30, 2013;
 posted February 21, 2013 (Doc. ID 176769); published April 12, 2013

Experiments for cell identification are presented using a high-precision cell phase measurement system that does not require any phase unwrapping. This system is based on a Mach-Zehnder interferometer using a phase-locking technique, and it measures the change in optical path length while the sample is scanned across the optical axis. The spatial resolution is estimated to be less than 1.1 μm . The sensitivity of optical path length difference is estimated to be less than 2 nm. Using experiments, we investigate the potential of this approach for cancer cell identification. In our preliminary experiments, cancer cells were distinguished from normal cells through comparison of optical path length differences. © 2013 Optical Society of America

OCIS codes: (120.5050) Phase measurement; (180.3170) Interference microscopy; (110.5086) Phase unwrapping; (170.4580) Optical diagnostics for medicine.

<http://dx.doi.org/10.1364/OL.38.001319>

Cancer cell identification by cell inspection is of great interest in cancer diagnosis. It has been shown that the index of refraction of cancer cells is relatively higher than normal cells [1,2], which makes precise cell phase measurement a good approach for quantitative diagnosis of a cell's condition. The quantitative phase provides important information about biological cells. Quantitative phase microscopes using interferometry have been explored to measure cell morphology information, including cell thickness and refractive index. These microscopes are based on various types of measurement methods [3–7]. However, these conventional systems need a phase unwrapping process when the measured phase objects are greater than 2π rad. Conventional phase unwrapping algorithm calculations may fail when the phase map has low intensity, a sharp rise or decline, or a high-spatial frequency. To improve precision and reduce errors in the phase unwrapping calculation, other approaches have been proposed [8,9], including multiple-wavelength techniques [10], phase retrieval in the spectral domain [11], and algorithms improvement [12].

Here, we present a high-precision phase measurement system that does not need phase unwrapping. We experimentally investigate the potential of this approach for cancer cell identification by distinguishing normal cells from cancerous cells through comparison of their optical path length differences. Unlike conventional phase microscopy, the proposed technique directly obtains the phase information by using an optical phase locking.

Figure 1 shows the optical setup of our phase measurement system based on a Mach-Zehnder interferometer with closed-loop feedback control. The beam from the He-Ne Laser is split by a polarized beam splitter (PBS). The sample is placed in the optical path of one of the arms of the interferometer. Microscopic objective lenses (MO, OBL-20, 0.4 NA, and SIGMA) are placed on each side of the sample. The other arm of the interferometer contains a mirror attached to a piezoelectric transducer (PZT, AE0505D08F, Thorlabs) to control the path length.

We assume that the intensity distribution results from the superposition of two waves by Mach-Zehnder interferometer. In the case where the two waves are of equal intensity, the distribution of optical intensity is given by

$$I(x, y) = I_0 \frac{1 + \cos\{\Delta\phi(x, y)\}}{2}, \quad (1)$$

$$\Delta\phi(x, y) = \frac{2\pi}{\lambda} \Delta L(x, y), \quad (2)$$

where I_0 is the light amplitude before the first beam splitter, λ is the wavelength, $\Delta\phi(x, y)$ is the phase difference, and $\Delta L(x, y)$ is the optical path length difference distribution. As previously noted, a phase unwrapping process is needed to measure optical paths longer than a wavelength. If the voltage applied to the PZT compensates the phase change of $\Delta\phi$, we have the condition of phase locking as

$$I(x, y) = I_0 \frac{1 + \cos\left\{\Delta\phi(x, y) - \frac{2\pi}{\lambda} \Delta L_{\text{pzt}}(x, y)\right\}}{2} = \text{const.} \quad (3)$$

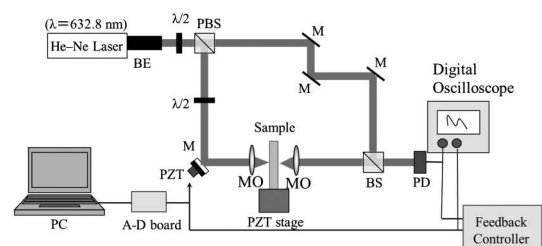


Fig. 1. Experimental setup. BE, beam expander; $\lambda/2$, half-wave plate; PBS, polarization beam splitter; M, Mirror; PZT, piezoelectric transducer; BS, beam splitter; and PD, photodetector.

Once the phase locking technique is employed, the interference fringe at the detector is locked by moving the mirror attached to the PZT. By using the value of the voltage applied to the PZT, it is possible to directly measure the $\Delta L(x, y)$ without any phase unwrapping processing. When a triangular voltage wave is applied to the PZT, the interference intensity becomes a sine wave. Assuming that the voltage applied to the PZT is proportional to the distance that the PZT moves, $\Delta L(x, y)$ is given by

$$\Delta L(x, y) = \frac{V_{\text{PZT}}(x, y) \times \lambda}{V_{\lambda}}, \quad (4)$$

where λ is the illumination wavelength, V_{λ} is the voltage change corresponding to one wavelength of PZT motion, and V_{PZT} is the voltage applied to the PZT. We calibrated the PZT devices, in advance, for using the calibration device, which is proportional to optical path difference. Based on the voltage value and the expression in Eq. (4), the optical path length difference is calculated. For a known thickness, the refractive index can be calculated. Conversely, if the refractive index is known, the thickness can be calculated.

In order to perform high-precision measurements, the modulation and synchronous detection are conducted from a point centered on a dark fringe to obtain a voltage proportional to the optical path length difference. To measure the microscopic region, the nearly collimated beam is focused by the first microscopic objective lens and then directed onto and through the sample. After passing through the sample, the modulated beam is collimated again by the second objective lens. The spatial resolution in the transverse direction is determined by the diameter of the focused beam, which is determined by the wavelength and by the NA ($n \sin \theta$) of the objective lens. In this experiment, an average spatial resolution of about $0.97 \mu\text{m}$ diameter is detected. To obtain the two-dimensional (2D) image, the sample is scanned by the PZT stage (P-157.2CL). Each optical element has been mounted on a vertical backboard. Thus, it is possible to reduce the influence of gravity on the measurement of the biological cell in the liquid. Line artifacts are sometimes caused along the scanning axis when the phase offset of the PZT occurred at the vertical axis that was scanned. We performed numerical line artifact correction for all measurement results.

For evaluating the phase sensitivity, we measured a planar light wave circuit (PLC). The specification of the PLC is the following: base material: silica, core size: $7 \mu\text{m}$, thickness of over-clad: $30 \mu\text{m}$, and refractive index of base material and clad n_2 : 1.458. The PLC consists of the over-clad of $30 \mu\text{m}$, the core size of $7 \mu\text{m}$, and a base material that has an equal refractive index as over-clad. The total thickness is 1.03 mm . The relative index difference is given by $\Delta n/n_1$, where relative index difference is 0.05%, n_2 is 1.458, and n_1 is calculated as 1.465. Therefore, Δn is 0.00733. Maximum optical path length difference is 52.0 nm because of oblique incidence. Figure 2(a) shows the measurement results of one-dimensional (1D) optical path length difference distribution. We have plotted the measurement results and the theoretical curve.

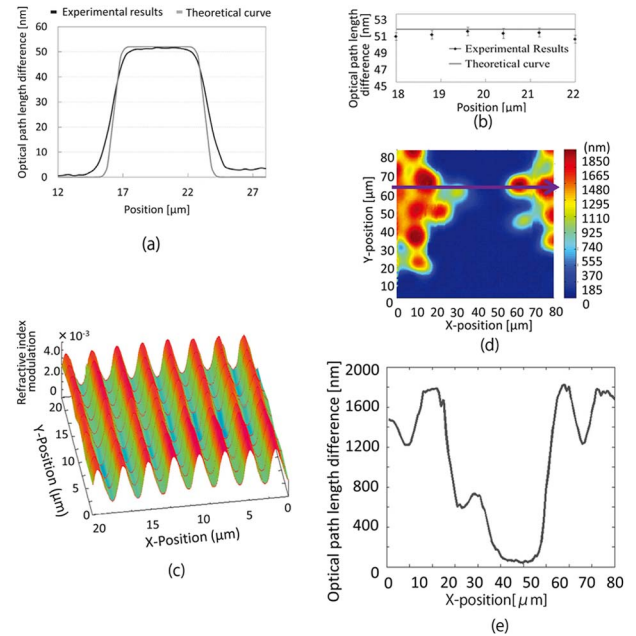


Fig. 2. Measurement of phase sensitivity and spatial resolution. (a) Experimentally obtained 1D optical path length difference of PLC. Both the measurement results and the theoretical curve are plotted. The black line is the average value, which was scanned 10 times. The gray line is the theoretical curve calculated using geometrical optics. (b) A zoomed-in version of the experiment results, showing the top area of the PLC. The plotted data represents the means \pm standard deviation ($n = 10$ times). (c) The result of the phase measurement. (d) Optical path length difference distribution for thick cells. (e) 1D optical path length difference of thick cells.

The solid line is the average value that was scanned 10 times. The gray line is the theoretical curve, calculated using geometrical optics. The standard deviation of each measurement point around the top of the PLC was less than 2 nm ($n = 10$ times in each measurement point), as shown in Fig. 2(b). This result proves that our system can measure the optical path length difference with an error less than 2 nm . For this reason, it is possible that the deviation is derived from the design value of the sample or measurement error. However, we cannot determine it in this study. Slope on both sides that is wider than the theoretical curve appears due to the effect of spherical aberration.

To illustrate the accuracy of the measurement, we present results with a volume-phase holographic (VPH) grating with a pitch of $2.2 \mu\text{m}$ ($29 \mu\text{m}$ thick). It was scanned in 2D over an area of $20 \mu\text{m} \times 20 \mu\text{m}$. Figure 2(c) shows the result of the phase measurement of the VPH grating. The refractive index variation was estimated from the sample thickness and the voltage variation with phase variation. A sine-wave refractive-index distribution with a $2.2 \mu\text{m}$ period was clearly obtained. This result illustrates that our phase measurement system has a high accuracy, close to the theoretically estimated spatial resolution of $0.97 \mu\text{m}$.

Now we show the measurement results of thick cells. Cells (5×10^5 cells) were centrifuged at 1500 rpm for 1 min in 15 ml centrifuge tube to form cellular pellets. After 1 day culture, the pellets were fixed with PBS

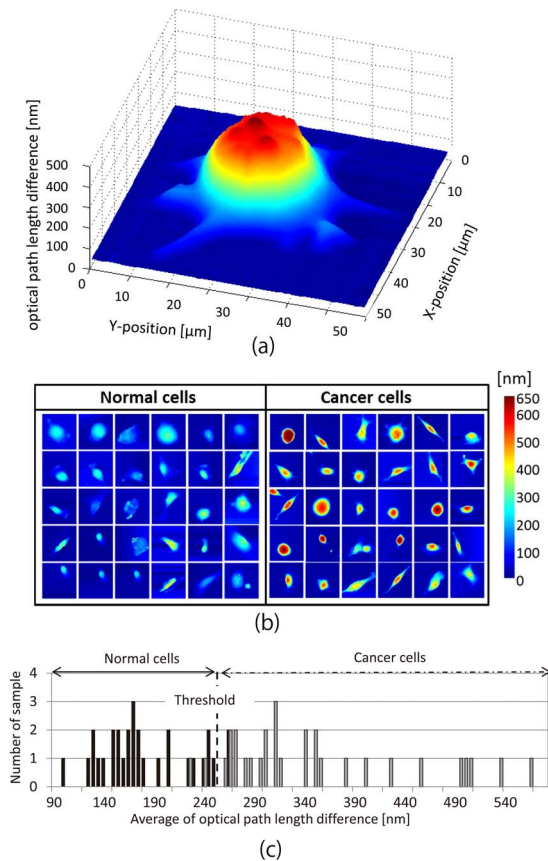


Fig. 3. (a) 3D optical path length difference distribution of a cancer cell, (b) optical path length difference distribution for normal cells, and (c) identification between normal and cancer cells. The horizontal axis shows the average of optical path length difference in the highest 2% of all data. The vertical axis shows the number of sample.

containing 0.1% glutaraldehyde for the observation. The samples have about three wavelength optical path length differences, which have a sharp rise and decline phase, as shown in Figs. 2(d) and 2(e). As far as we investigated, we never find fine microscopic cell images that have about three wavelength optical path length difference more accurate than our measurement results.

Next we used this system for cancer cell identification. Breast cancer cells, MDA-MB-231 [American Type Culture Collection (ATCC), Manassas, VA] and MCF-7 [Health Science Research Resources Bank, Osaka, Japan] and breast benign cells, MCF-10A (as normal cell model, ATCC), were cultured on glass slide in Dulbecco's Modified Eagle/Nutrient Mixture F-12 (DMEM/F-12, Invitrogen, Carlsbad, CA) medium containing 10% fetal bovine serum for 2 days and then fixed with 0.1% glutaraldehyde. The biological samples were sandwiched between two glass slides with spacers. The thickness of the glass is 500 μm , and the thickness of the spacer is 50 μm . Thus, the sample remains in an accurate position as well as retaining moisture. First, the 2D phase distribution as the voltage of PZT is obtained through optical scanning. The data size is 100×100 pixels. The measurement time is 100 s per frame. Figure 3(a) shows a three-dimensional (3D) optical path length difference distribution of a

cancer cell. The central part of the 3D optical path length difference of cancer exhibits a nucleiform. In addition, even though we used a coherent laser there is very little speckle noise in our measurement results.

We measured 30 normal cells and 30 cancer cells. When the averages of the optical path length difference in the highest 2% of optical path length difference distribution are plotted, we can distinguish cancer cells from normal cells. If the threshold value of average optical path length difference is set at 260 nm, the number of false negatives is two and the number of false positives is two, as shown in Fig. 3(c). The experimental results indicate that the cancer cells were associated with higher optical path length difference than that of the normal cells. Cancer cells often appear in ascites of cancerous patients, such as in ovarian cancer, which leads to peritoneal metastasis. To examine the cancer and its metastasis, paracentesis abdominis is often performed to detect cancer cells. Our technique can identify between normal and cancer cells. It is expected that our technique can be applied for the detection of the cancer cells in ascites in cancer clinic.

In summary, a high-dynamic-range phase measurement system that does not need unwrapping processing is used for cancer cell identification. The important property of our system is that it can measure transparent objects without using the phase unwrapping process even if the thickness of the object is more than one wavelength. Our system can provide the quantitative phase information with high accuracy and it may be used for advanced cell analyses, such as quality control and functional inspection of cells.

This study is partly supported by the Cooperative Program of Japan Science and Technology Agency. The authors would like to acknowledge Prof. K. Kodate at Japan Woman's University, Dr. J. Mizuno at Photonic System Solutions Inc. for valuable discussions throughout this work.

References

- W. J. Choi, D. I. Jeon, S. Ahn, J. Yoon, S. Kim, and B. H. Lee, *Opt. Express* **18**, 23285 (2010).
- P. Massatsch, F. Charrière, E. Cuche, P. Marquet, and C. D. Depeursinge, *Appl. Opt.* **44**, 1806 (2005).
- G. Pedrini and H. J. Tiziani, *Appl. Opt.* **41**, 4489 (2002).
- P. Ferraro, D. Alferi, S. D. Nicola, L. D. Petrocellis, A. Finizio, and G. Pierattini, *Opt. Lett.* **31**, 1405 (2006).
- I. Yamaguchi, J. Kato, S. Ohta, and J. Mizuno, *Appl. Opt.* **40**, 6177 (2001).
- B. Grajciar, Y. Lehareinger, A. F. Fercher, and R. A. Leitgeb, *Opt. Express* **18**, 21841 (2010).
- P. Marquet, B. Rappaz, P. Magistretti, E. Cuche, Y. Emery, T. Colomb, and C. Depeursinge, *Opt. Lett.* **30**, 468 (2005).
- P. Gao, B. Yao, J. Han, L. Chen, Y. Wang, and M. Lei, *Appl. Opt.* **47**, 2760 (2008).
- G. Páez and M. Strojnik, *J. Opt. Soc. Am. A* **16**, 475 (1999).
- A. Khmaladze, R. L. Matz, C. Zhang, T. Wang, M. M. B. Holl, and Z. Chen, *Opt. Lett.* **36**, 912 (2011).
- J. Zhang, B. Rao, L. Yu, and Z. Chen, *Opt. Lett.* **34**, 3442 (2009).
- S. Yuqing, *Opt. Express* **15**, 8059 (2007).